IEEE Access
Multidisciplinary | Rapid Review | Open Access Journal

Received March 4, 2021, accepted April 3, 2021, date of publication April 8, 2021, date of current version April 16, 2021.

Digital Object Identifier 10.1109/ACCESS.2021.3071821

Improved Seamless Switching Control Strategy for AC/DC Hybrid Microgrid

GUISHUO WANG, (Fellow, IEEE), XIAOLI WANG, AND XIANG GAO
School of Mechanical, Electrical and Information Engineering, Shandong University, Weihai 264209, China
Corresponding author: Xiang Gao (gaoxiang@sdu.edu.cn)

ABSTRACT Aiming at the problems of transient over-current and over-voltage in the switching process of AC/DC hybrid microgrid in grid-connected mode and island mode, which leads to the sudden change of transmission power and seriously affects the power transmission quality. In this paper, an improved seamless switching control strategy of droop control with disturbance observer is designed. The main work is as follow: according to the diffident power transmission calculation methods of droop control in grid-connected mode and island mode, the adaptive switching is realized by detecting the current and frequency at Point of Common Coupling(PCC) of public power grid. Secondly, the switching from island mode to grid-connected mode will cause impact due to the difference of frequency, phase and amplitude between microgrid and public grid, and even cause system collapse. So the pre-synchronization control of frequency, phase and amplitude is designed. Based on the droop control, the disturbance observation(DOB) is added, which can quickly track the sudden change of system current, and suppress the sudden change by the difference between the tracking value and the actual value, so as to realize the smooth switching from island to grid. Finally, the effectiveness and feasibility of the control strategy are verify in Matlab/Simulink.

INDEX TERMS AC/DC hybrid microgrid, droop control, seamless switching, disturbance observation.

I. INTRODUCTION

In recent years, with the large increase of renewable resources such as solar energy and wind energy in distributed generation(DG) units, the concept of microgrid has been gradually taken into account. As a new distribution scheme in microgrid, AC/DC hybrid microgrid integrates DG and energy storage system(ESS) more effectively to provide efficient and reliable power supply for both loads [1]. AC/DC hybrid microgrid is usually composed of AC sub-microgrid, DC sub-microgrid and bidirectional AC/DC converters(BIC). BIC plays an important role in maintaining the voltage stability of AC/DC bus and realizing the bidirectional energy flow as the medium of two sub-microgrids [2].

The AC/DC hybrid microgrid can be divided into grid-connected mode and island mode according to whether it is connected to the public grid through PCC or not. In grid-connected mode, the system voltage of the AC sub-microgrid is supported by the public grid, and the BIC mainly maintains the DC bus voltage stability and power balance in the system [3]. In island mode, the AC sub-microgrid loses the support of the public grid, and the BIC needs to maintain the AC/DC bus stability and power balance within the system [4]. When the public grid fails or needs to be repaired, in order not to affect the normal operation of the AC/DC hybrid microgrid, it is necessary to disconnect from public grid, and wait for the failure to be repaired before reconnecting to the public grid. However, in the process of mode switching, due to the different of phase, frequency and amplitude, transient over-current is generated, which causes power sudden change and seriously affects power system security [5]. Therefore, how to formulate a reasonable control strategy for BIC to achieve seamless switching between grid-connected mode and island mode is still an important topic.

In order to ensure seamless switching between grid-connected mode and island mode, many scholars have proposed various constructive methods. In reference [6], [7], the control modes of the converter in different modes are analyzed. The P/Q control is used in the grid-connected mode and V/F control is used in the island mode. Because of the change of control algorithm, fast switching is required, but it is easy to produce transient impact. The frequency modulation characteristics of droop control analogue generator set are easy to achieve power equalization, and gradually become the mainstream of BIC control. It is process of switching between

The associate editor coordinating the review of this manuscript and approving it for publication was Ali Raza.

grid-connected mode and island mode, droop control is more advantageous without switching control algorithms [8], [9]. However, it is difficult to achieve smooth transition during modes switching only by relying on traditional droop control strategies. In reference [10], the idea of hierarchical control, combined with droop control. It not only achieves seamless switching between island mode and grid-connected mode, but also has plug and play of load unit and circuit recovery capability. However, the pre-synchronization period of island mode to grid-connected mode switching is too long, resulting in frequency impact exceeding 0.5 Hz during the pre-synchronization process. In reference [11], designs a smooth state transition autonomous control strategy based on droop control. This method is based on the non-linear algorithm and the interface of electromagnetic transient simulation to find optimal control parameters to minimize the voltage deviation of mode switching. Although the voltage deviation decreases, the power transmission shows a large jitter over a period of time and does not want to achieve the desired effect. In reference [12], on the basis of droop control, the output current feed-forward and the container current feedback are added, which reduces the instantaneous over-current during switching and compensates the transient pressure drop to alleviate interference and improve the dynamic performance of the system. Although interference during mode switching can be suppressed, the size and duration of the bias depend on the performance of the controller. In order to limit the size and duration of the bias to an acceptable range, the voltage controller must provide greater damping.

Through the analysis of existing seamless switching control strategies, this paper designs a seamless switching improved control strategy. When the grid-connected mode is switched to the unplanned island mode, the occurrence of unplanned islands can be detected effectively, and the reference power calculation mode can be switched in a short time. The phase, frequency and voltage amplitude pre-synchronization control is designed to avoid the system crash due to the component differences between the microgrid system and the public grid. Finally, the current inner loop control based on DOB is designed to suppress the impact caused by mode switching, and the switching between grid-connected mode and island mode is achieved.

The rest of this paper is as follow: Section 2 introduces the system structure and droop control strategy of AC/DC hybrid microgrid. Section 3 introduces the basic principle of the DOB. Section 4 describes the control methods involved in mode switching. Section 5 verifies the method designed in this paper by simulation. Section 6 summarizes the whole paper.

II. STRUCTURE AND CONTROL METHOD OF MICROGRID SYSTEM

A. MICROGRID SYSTEM STRUCTURE

The AC/DC hybrid microgrid structure used in this paper is typical topology I structure in Fig. 1. It is composed of AC sub-microgrid, DC sub-microgrid and BIC. The AC sub-microgrid is connected to the public grid through PCC. The DC sub-microgrid is composed of PV, ESS and AC load. PV is connected to DC bus by DC/DC converter, and ESS is connected to DC bus by bidirectional DC/DC converter. The composition of AC sub-microgrid is the same as that of DC sub-microgrid. PV and ESS are connected to the AC bus through DC/AC converter on the basis of DC/DC converter. BIC can exchange energy between two sub-microgrid by connecting AC bus and DC bus.

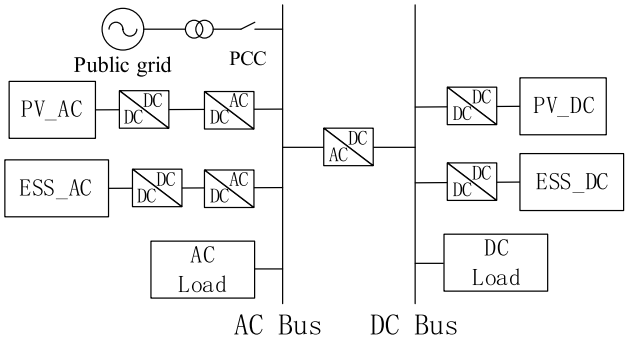

FIGURE 1. System topology of AC/DC hybrid microgrid.

B. DROOP CONTROL

This droop control circuit is shown Fig. 2.

The BIC uses a droop control method to achieve a reasonable allocation of energy between AC and DC sub-microgrids, while ensuring a reasonable allocation of load consumption power within the system. Compared with P/Q control and V/F control, droop control is applicable in both island mode and grid-connected mode, so there is no need to switch control mode when switching between grid-connected mode and island mode.

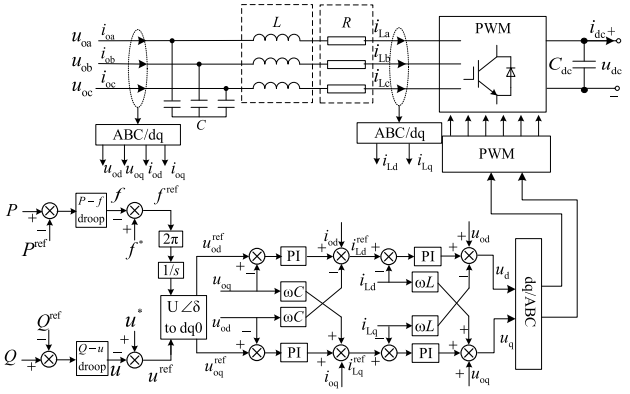

FIGURE 2. Droop control topological circuit.

In the droop control mode, the AC sub-microgrid bus frequency and voltage amplitude reflect the output active power and reactive power in the AC sub-microgrid respectively, which meet the $P_{ac} - f_{ac}$ and $Q_{ac} - u_{ac}$ droop characteristics, as shown in Fig. 3.

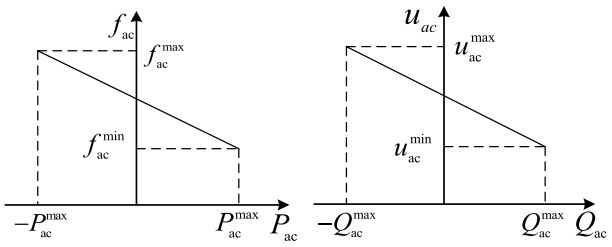

FIGURE 3. Droop characteristic curves of $P_{ac} - f_{ac}$ and $Q_{ac} - u_{ac}$.

According to Fig. 3, the droop characteristics of $P_{ac} - f_{ac}$ and $Q_{ac} - u_{ac}$ can be expressed as fellow:

$$\begin{cases} f_{ac} = f_{ac}^{ref} - m(P_{ac} - P_{ac}^{ref}) \\ u_{ac} = u_{ac}^{ref} - n(Q_{ac} - Q_{ac}^{ref}) \end{cases}. \tag{1}$$

where, m and n are the active power and reactive power droop coefficient, f_{ac}^{ref} and u_{ac}^{ref} are the bus frequency and voltage amplitude ratings of the AC sub-microgrid, P_{ac}^{ref} and Q_{ac}^{ref} are the active power and reactive power ratings.

There is no consumption of reactive power in the DC sub-microgrid. The DC sub-microgrid bus directly reflects the output power in the DC sub-microgrid and satisfies the $P_{dc} - u_{dc}$ droop characteristic, as shown in Fig. 4.

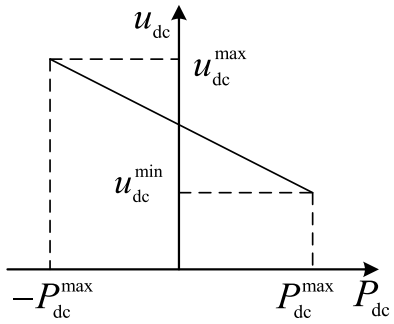

FIGURE 4. Droop characteristic curves of $P_{dc} - u_{dc}$.

$P_{dc} - u_{dc}$ droop characteristics can be expressed as:

$$u_{dc} = u_{dc}^{ref} - k(P_{dc} - P_{dc}^{ref}), \tag{2}$$

where, u_{dc}^{ref} is DC sub-microgrid bus voltage rating, k is the active power droop coefficient, P_{dc}^{ref} is DC sub-microgrid active power rating.

When calculating the reference value of reactive power in the whole system, there is reactive power in the DC sub-microgrid. Therefore, the calculation of the reference value of the reactive power does not need to be compared between the parameters of the two sub-microgrids, but can be calculated directly. When calculating the active power reference value in the system, it is not possible to directly compare the AC sub-microgrid frequency with DC sub-microgrid voltage unit level and interval. In order to better measure the output of AC and DC sub-microgrids, the frequency of AC sub-microgrid and DC sub-microgrid voltage need to be compared under the same coordinate system. By increasing the threshold setting, the AC sub-microgrid transmission reference active power is obtained as follows:

$$P_{ac}^{*} = \begin{cases} P_{BIC}^{*} & f_{ac} > f_{ac,Hmax} \\ P_{BIC}^{*} \dfrac{f_{ac} - f_{ac,Hmin}}{f_{ac,Hmax} - f_{ac,Hmin}} & f_{ac,Hmin} \le f_{ac} \le f_{ac,Hmax} \\ 0 & f_{ac,Lmin} \le f_{ac} \le f_{ac,Hmin} \\ -P_{BIC}^{*} \dfrac{f_{ac} - f_{ac,Lmin}}{f_{ac,Lmax} - f_{ac,Lmin}} & f_{ac,Lmax} \le f_{ac} \le f_{ac,Lmin} \\ -P_{BIC}^{*} & f_{ac} < f_{ac,Lmax} \end{cases}, \tag{3}$$

where, P_{BIC}^{*} is rated value of the active power transmitted by the BIC, $f_{ac,Hmin}$ is the minimum value of the upper threshold setting for the BIC, $f_{ac,Hmax}$ is the maximum value of the upper threshold setting for the BIC, $f_{ac,Lmin}$ is the minimum value of the lower threshold setting and $f_{ac,Lmax}$ is the maximum value of the lower threshold setting.

The reference active power for DC sub-microgrid transmission is as follows:

$$P_{dc}^{*} = \begin{cases} P_{BIC}^{*} & u_{dc} > u_{dc,Hmax} \\ P_{BIC}^{*} \dfrac{u_{dc} - u_{dc,Hmin}}{u_{dc,Hmax} - u_{dc,Hmin}} & u_{dc,Hmin} \le u_{dc} \le u_{dc,Hmax} \\ 0 & u_{dc,Lmin} \le u_{d'c} \le u_{dc,Hmin} \\ -P_{BIC}^{*} \dfrac{u_{dc} - u_{dc,Lmin}}{u_{dc,Lmax} - u_{dc,Lmin}} & u_{dc,Lmax} \le u_{d'c} \le u_{dc,Lmin} \\ -P_{BIC}^{*} & u_{dc} < u_{dc,Lmax} \end{cases}, \tag{4}$$

where, $u_{dc,Hmin}$ is the minimum value of the upper threshold setting for BIC, $u_{dc,Hmax}$ is the maximum value of upper threshold setting for BIC, $u_{dc,Lmin}$ is the minimum value of the lower threshold setting, and $u_{dc,Lmax}$ is the maximum value of the lower threshold setting. Thus, the reference active power for BIC transmission in island mode is obtained:

$$P_{BIC}^{ref} = 0.5(P_{dc}^{*} - P_{ac}^{*}). \tag{5}$$

By comparing the sizes of P_{dc}^{*} and P_{ac}^{*}, the bidirectional flow of active power of BIC is achieved according to the idea of equalization. The DC sub-microgrid is the positive reference direction to the AC sub-microgrid. When $P_{dc}^{*} > P_{ac}^{*}$, the BIC is in the inverted state. When $P_{dc}^{*} = P_{ac}^{*}$, the BIC is in standby. When $P_{dc}^{*} < P_{ac}^{*}$, the BIC is in the rectifying state.

When AC/DC hybrid microgrid is running in grid-connected mode, the frequency of AC sub-microgrid is rated at 50Hz, which is supported by the public grid. At this time, if DC sub-microgrid has surplus power, it will flow into the public grid through the BIC. Similarly, due to the power deficit of the DC sub-microgrid, the public grid flows into the DC sub-microgrid through the BIC. Then, the BIC transmission reference active power in the grid-connected modes is as follows:

$$P_{BIC}^{ref} = P_{dc}^{*}. \tag{6}$$

The difference between the active power reference value and the reactive power reference value is obtained by comparing them with the actual value. The frequency and voltage amplitude that need to be adjusted are obtained by the droop control. The reference voltage of d-axis and q-axis in two rotating coordinate systems is obtained by three-phase voltage synthesis and park transformation into the voltage and current control link.

According to Kirchhoff's law, the mathematical model in d-q coordinate system is obtained:

$$\begin{cases} L\dfrac{di_{\mathrm{Ld}}}{dt} + Ri_{\mathrm{Ld}} = u_{\mathrm{od}} - u_{\mathrm{d}} - \omega Li_{\mathrm{Lq}} \\ L\dfrac{di_{\mathrm{Lq}}}{dt} + Ri_{\mathrm{Lq}} = u_{\mathrm{oq}} - u_{\mathrm{q}} + \omega Li_{\mathrm{Ld}} \\ C\dfrac{du_{\mathrm{od}}}{dt} = i_{\mathrm{od}} - i_{\mathrm{Ld}} - \omega Cu_{\mathrm{oq}} \\ C\dfrac{du_{\mathrm{oq}}}{dt} = i_{\mathrm{oq}} - i_{\mathrm{Lq}} + \omega Cu_{\mathrm{od}} \end{cases} . \tag{7}$$

It can be seen from the above equation that there is coupling in the system. In order to simplify the design of the control system and realize decoupling control, when the voltage outer loop is defined as:

$$\begin{cases} i_{\mathrm{Ld}}^{\mathrm{ref}} = (u_{\mathrm{od}}^{\mathrm{ref}} - u_{\mathrm{od}})(k_{\mathrm{up}} + \dfrac{k_{\mathrm{ui}}}{s}) - \omega Cu_{\mathrm{oq}} + i_{\mathrm{od}} \\ i_{\mathrm{Lq}}^{\mathrm{ref}} = (u_{\mathrm{oq}}^{\mathrm{ref}} - u_{\mathrm{oq}})(k_{\mathrm{up}} + \dfrac{k_{\mathrm{ui}}}{s}) + \omega Cu_{\mathrm{od}} + i_{\mathrm{oq}} \end{cases} , \tag{8}$$

where, k_{up} and k_{ui} are proportional integral coefficients of PI controller in outer voltage loop respectively, $u_{\mathrm{od}}^{\mathrm{ref}}$ and $u_{\mathrm{oq}}^{\mathrm{ref}}$ are the reference voltage of d-axis and q-axis. The inner loop is current loop, and the output voltage of d-axis and q-axis of BIC can be obtained by PI controller. Due to the existence of d-q cross coupling term in the system, feedforward compensation is added to eliminate the influence of cross coupling and realize current decoupling control. For the convenience of decoupling, the mathematical model of current inner loop is as follows:

$$\begin{cases} u_{\mathrm{d}} = -(k_{2\mathrm{p}} + \dfrac{k_{2\mathrm{i}}}{s})(i_{\mathrm{Ld}}^{\mathrm{ref}} - i_{\mathrm{Ld}}) + u_{\mathrm{od}} - \omega Li_{\mathrm{Lq}} \\ u_{\mathrm{q}} = -(k_{2\mathrm{p}} + \dfrac{k_{2\mathrm{i}}}{s})(i_{\mathrm{Lq}}^{\mathrm{ref}} - i_{\mathrm{Lq}}) + u_{\mathrm{oq}} + \omega Li_{\mathrm{Ld}} \end{cases} , \tag{9}$$

where, $k_{2\mathrm{p}}$ and $k_{2\mathrm{i}}$ are the proportional coefficient and integral coefficient of PI controller in current inner loop respectively, $i_{\mathrm{Ld}}^{\mathrm{ref}}$ and $i_{\mathrm{Lq}}^{\mathrm{ref}}$ are the reference current of d-axis and q-axis inductor respectively. Finally, the d-axis and q-axis voltages are obtained, and the control waveform of BIC is obtained by park invers transformation, and then the three-phase voltage output of BIC is obtained by pulse width modulation(PWM).

III. PRINCIPLE OF DISTURBANCE OBSERVER

When switching between grid-connected mode and island mode, it will lead to power mutation, which will cause large deviation of AC/DC bus voltage and frequency, and seriously affect the stability of microgrid system. Therefore, the disturbance observer is added to quickly track the disturbance current caused by power mutation and eliminate the disturbance before feedback. The basic idea of DOB is to take the difference between the actual variable and the reference variable produce by the external disturbance and the change of model parameters as the equivalent control input to obtain the equivalent disturbance value. Finally, equal compensation is introduced into the control system to suppress the interference. The principle of DOB is shown in Fig. 5 [13].

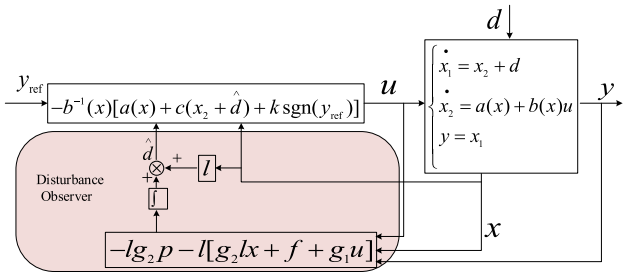

FIGURE 5. Structure of disturbance observer system.

It can be seen from Fig. 5 that the DOB is composed of the system control link and the disturbance observation link. According to the reference value of input, the system control realizes the accurate tracking of system output variables. The control system can be express as:

$$\begin{cases} \dot{x} = f + g_1u + g_2d \\ y = x_1 \end{cases} , \tag{10}$$

where, u is the input, d is the external disturbance, and y is the output of the system. The mathematical model of DOB is as follows:

$$\begin{cases} \dfrac{dp}{dt} = -lg_2p - l[g_2lx + f + g_1u] \\ \hat{d} = p + lx \end{cases} , \tag{11}$$

where, $\hat{d}$ is the disturbance estimate, p is the internal state of the disturbance observer, l is the gain of the observer $l = [l_1, l_2, \cdots l_n]$, and x is the state variable of the system. f, g_1 and g_2 are functions of x as follows:

$$\begin{cases} x = [x_1, x_2]^{\mathrm{T}} \\ f = [x_2, a(x)]^{\mathrm{T}} \\ g_1(x) = [1, 0]^{\mathrm{T}} \\ g_2(x) = [0, b(x)]^{\mathrm{T}} \end{cases} . \tag{12}$$

In the system control, the disturbance estimation a should satisfy the follow equation:

$$\lim_{t\to\infty} \frac{d}{dt} d = 0. \tag{13}$$

Under the above conditions, if the gain l of the DOB remains $lg_2 > 0$, then the disturbance estimate $\hat{d}$ of the system is approximately equal to the actual disturbance d of the system. Therefore, the error convergence equation of disturbance observation link can be expressed as:

$$\frac{de(t)}{dt} + lxg_2e(t) = 0. \tag{14}$$

where, $e(t)$ is the disturbance error, which can be expressed as $e(t) = d - \hat{d}$. At this time, the system is globally asymptotically stable and the disturbance can be accurately tracked.

IV. SEAMLESS SWITCHING CONTROL STRATEGY

When AC/DC hybrid microgrid switching between grid-connected mode and island mode, the frequency, phase and voltage amplitude different in the system will not affect the stability of the system, so the seamless switching can be realized. Model switching is divided into grid-connected mode switching to island mode and island mode switching to grid-connected mode. Switching from grid-connected mode to island mode can be divided into planned island and unplanned island. In view of the above situation, this paper analyzes and design relevant strategies.

A. SWITCHING FORM GRID-CONNECTED MODE TO ISLAND MODE

Switching from grid-connected to planned island mode or island mode to grid-connected mode is set in advance and can be adjusted according to the setting. However, the transition from grid-connected to unplanned island is an unpredictable failure such as public grid failure under unknow conditions, which leads to the disconnection between microgrid system and public grid, which is sudden [14]. Therefore, the research of switching from grid-connected mode to island mode mainly analyzes and studies the switching from grid-connected mode to unplanned island mode.

When the public grid fails, the connection point at PCC is disconnected, which leads to the unplanned island of AC/DC hybrid microgrid. Because of the suddenness, it is necessary for the system to detect the occurrence of unplanned island mode and switch the power calculation mode autonomously in order to maintain the system stability effectively. When the unplanned island mode occurs, the power calculation mode is not switched to the island mode, so the power is still transmitted or absorbed to the AC side, resulting in power disorder in the system. The mode switch detection process is as follows:

During the operation of AC/DC hybrid microgrid, unplanned island is detected continuously. When the current of public grid at PCC is all zero, it can be divided into two case. Firstly, the power consumed by the load in the AC/DC hybrid microgrid system is equal to power in the system. In this case, the current in the microgrid system will not be transmitted to the public grid theoretically, so the three-phase current at PCC is about 0. However, because there are errors in the calculation of each component, the minimum current can still be detected. Secondly, the PCC is disconnected, and the three-phase current of the public grid at PCC is constant at 0. In order to better judge, the frequency of AC/DC hybrid microgrid is judged. If $49.99 < f < 50.01$, it means that the frequency is about 50 Hz and it is still in grid-connected operation. Otherwise, if the fluctuation exceeds this range, it means that without the support of the public grid, there will be excessive or insufficient power and unplanned island. When the unplanned island is detected, the BIC power calculation mode from grid-connected to island mode, and the switch from grid-connected to island mode is completed. The conversion from unplanned island mode to grid-connected mode is the same.

B. FORM ISLAND MODE TO GRID-CONNECTED MODE

When the public grid fault repair or maintenance is completed, AC/DC hybrid microgrid needs to re-connected to the public grid. However, in island mode, the frequency, phase and voltage amplitude of AC/DC hybrid microgrid are quite different from those of public grid. Direct connection will produce transient over-current and voltage, which will lead to power mutation and seriously affect the stability and security of power grid system [15]. Therefore, before closing the PCC grid connected switch, pre-synchronization operation is needed to realize the accurate matching of frequency, phase and voltage amplitude between microgrid and public grid, so as to prevent the impact caused by transient. The pre-synchronization control is shown in Fig. 7.

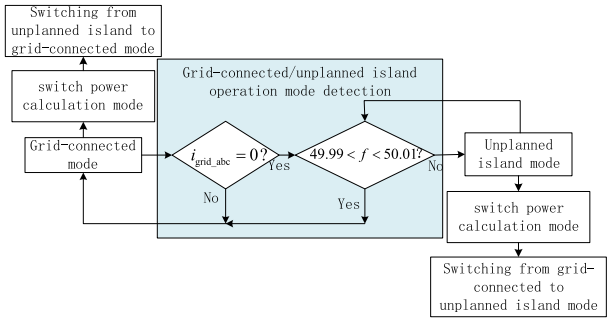

FIGURE 6. Grid-connected/unplanned island operation mode detection process.

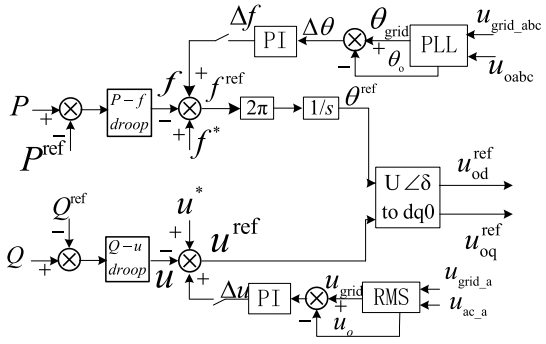

FIGURE 7. Pre-synchronization control.

To achieve pre-synchronization, it is necessary to detect the frequency, phase and voltage amplitude of BIC and public grid. The difference of synchronization frequency is calculated as follows:

$$\Delta f = (k_{p\theta} + \frac{k_{i\theta}}{s})(\theta_{grid} - \theta_o), \tag{15}$$

where, $k_{p\theta}$ and $k_{i\theta}$ are the proportional and integral coefficients of PI controller, θ_{grid} and θ_o are PLL to detect the

phase of public grid and AC bus. The difference of pre-synchronization voltage amplitude is as follows:

$$\Delta u = (k_{\mathrm{pu}} + \frac{k_{\mathrm{iu}}}{s})(u_{\mathrm{grid}} - u_{\mathrm{o}}), \tag{16}$$

where, u_{grid} and u_{o} are the voltage amplitudes calculated by RMS after PLL detects the public and AC bus respectively.

Combining equation (15) and equation (16), the mathematical model of island mode droop control in pre-synchronization link is obtained as follows:

$$\begin{cases} f^{\mathrm{ref}} = f^* - m(P - P^{\mathrm{ref}}) + (k_{\mathrm{p}\theta} + \dfrac{k_{\mathrm{i}\theta}}{s})(\theta_{\mathrm{grid}} - \theta_{\mathrm{o}}) \\ u^{\mathrm{ref}} = u^* - n(Q - Q^{\mathrm{ref}}) + (k_{\mathrm{pu}} + \dfrac{k_{\mathrm{iu}}}{s})(u_{\mathrm{grid}} - u_{\mathrm{o}}) \end{cases}. \tag{17}$$

When the frequency, phase and voltage amplitude errors between the BIC and the public grid are detected in the pre-synchronization link, the following conditions are met [16]:

$$\begin{cases} \Delta f < 0.5\,\mathrm{Hz} \\ \Delta\theta < 1^\circ \\ \Delta u < 7\%\,\mathrm{V} \end{cases}. \tag{18}$$

At this time, the switch at PCC is closed, the reference power of droop control strategy is switched from island mode to grid-connected mode, and the grid-connected operation is realized, and the pre-synchronization is completed.

C. INNER LOO DESIGN BASED ON DISTURBANCE OBSERVER

The reference voltage is synthesized by the power loop and is controlled by the inner loop of voltage and current. The voltage and current components in the inner loop are DC variables, so they meet the requirements of $\lim_{t\to\infty} \frac{d}{dt} d = 0$. When the power mutation occurs in AC/DC hybrid microgrid system, it is caused by transient change of output current in BIC and fluctuation of bus voltage. Therefore, the DOB is added in the current loop to solve the problem of current and voltage impact in the case of power mutation, and disturbance suppression compensation control is carried out to realize the smooth transition of power in the system [17]. The inner loop design structure based on DOB is shown in Fig. 8.

In Fig. 8, the calculation methods of d-axis and q-axis are similar, and the d-axis current loop is used for analysis. If the d-axis current and voltage components are brought into the DOB for calculation, the deformation of equation (12) is as follows:

$$\begin{cases} x = [x_1, x_2]^{\mathrm{T}} = [i_{\mathrm{Ld}}, u_{\mathrm{od}}]^{\mathrm{T}} \\ f = [x_2, a(x)]^{\mathrm{T}} = [-\dfrac{Ri_{\mathrm{Ld}}}{L} + \dfrac{u_{\mathrm{od}}}{L} - \omega i_{\mathrm{Lq}}, \\ \quad -\dfrac{i_{\mathrm{Ld}}}{C} - \omega u_{\mathrm{oq}}]^{\mathrm{T}} \\ g_1(x) = [1, 0]^{\mathrm{T}} = [-\dfrac{1}{L}, 0]^{\mathrm{T}} \\ g_2(x) = [0, b(x)]^{\mathrm{T}} = [0, \dfrac{1}{C}] \end{cases}, \tag{19}$$

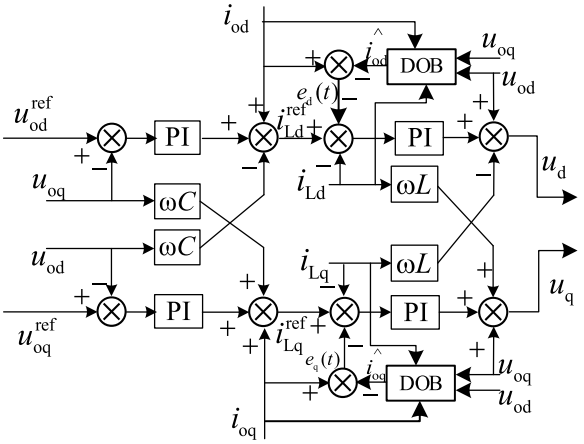

FIGURE 8. Current inner loop control based on DOB.

where, R, L and C are the three-phase filter resistance, inductance and capacitance at AC side of BIC.

The components in the above equation are brought into the control system as follows:

$$\begin{cases} u = u_{\mathrm{d}} \\ d = i_{\mathrm{od}} \\ \dot{x} = f + g_1 u + g_2 d \\ = [-\dfrac{Ri_{\mathrm{Ld}}}{L} + \dfrac{u_{\mathrm{od}}}{L} - \omega i_{\mathrm{Lq}}, -\dfrac{i_{\mathrm{Ld}}}{C} - \omega u_{\mathrm{oq}}]^{\mathrm{T}} \\ +[-\dfrac{1}{L}, 0]^{\mathrm{T}} \cdot u_{\mathrm{d}} + [0, \dfrac{1}{C}] \cdot i_{\mathrm{od}} \\ y = x_1 = i_{\mathrm{Ld}} \end{cases}. \tag{20}$$

The disturbance current of d-axis disturbance observation link is obtained as follows:

$$\begin{cases} \dfrac{dp}{dt} = -lg_2 p - l[g_2 lx + f + g_1 u] \\ = -\dfrac{l_{\mathrm{d}}}{C} p - \dfrac{l_{\mathrm{d}}^2}{C} u_{\mathrm{od}} + \dfrac{i_{\mathrm{Lq}}}{C} l_{\mathrm{d}} - \omega u_{\mathrm{oq}} l_{\mathrm{d}} \\ \hat{i}_{\mathrm{od}} = p + l_{\mathrm{d}} u_{\mathrm{od}} \end{cases}, \tag{21}$$

where $l = [0, l_{\mathrm{d}}]$, the value of l_{d} should not be too large, otherwise the observation system will be saturated. To sum up, the mathematical model based on the inner current loop of disturbance observer can be expressed as follows:

$$\begin{cases} u_{\mathrm{d}} = -(k_{2\mathrm{p}} + \dfrac{k_{2\mathrm{i}}}{s})[(i_{\mathrm{Ld}}^{\mathrm{ref}} - i_{\mathrm{Ld}}) - (i_{\mathrm{od}} - \hat{i}_{\mathrm{od}})] \\ +u_{\mathrm{od}} - \omega L i_{\mathrm{Lq}} \\ u_{\mathrm{q}} = -(k_{2\mathrm{p}} + \dfrac{k_{2\mathrm{i}}}{s})[(i_{\mathrm{Lq}}^{\mathrm{ref}} - i_{\mathrm{Lq}}) - (i_{\mathrm{oq}} - \hat{i}_{\mathrm{oq}})] \\ +u_{\mathrm{oq}} + \omega L i_{\mathrm{Ld}} \end{cases}. \tag{22}$$

V. SIMULATION VERIFICATION OF CONTROL STRATEGY

In the process of grid connected/island mode switching, due to the difference of frequency, phase and voltage amplitude between AC/DC hybrid microgrid system and public grid, impact occurs during mode switching, which affects the stability of the system. In this paper, the unplanned island detection is set in the process of grid-connected mode to

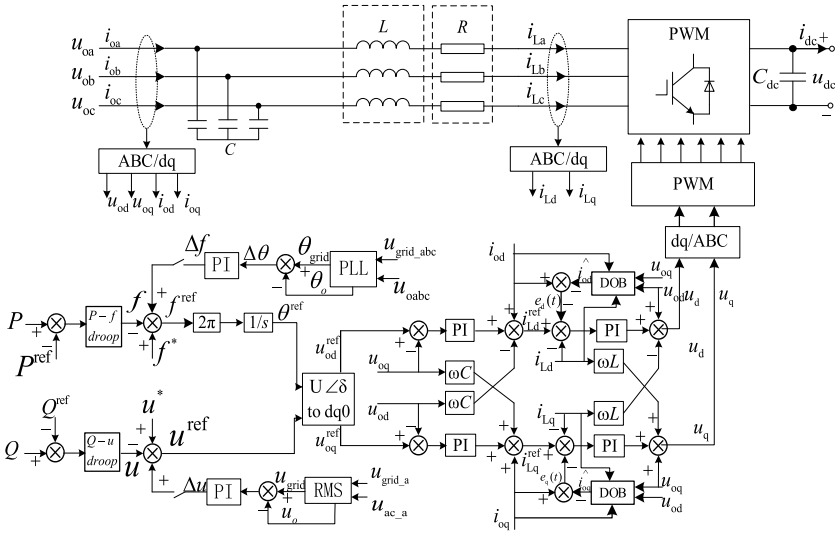

FIGURE 9. Improved seamless switching control structure for BIC.

unplanned island mode. When the unplanned island occurs, the power calculation mode switching in the control strategy can be completed without human intervention. In the process of switching from island mode to grid-connected mode, the pre-synchronization control is designed to realize the synchronization of frequency, phase and voltage amplitude between microgrid and public grid in island mode, which reduces the impact of mode switching process. Aiming at the impact problem caused by transient over-current in mode switching, a current inner loop based on DOB is designed. By tracking the difference value of disturbance current through disturbance estimation value, the abrupt variables in mode switching process are compensated, and seamless switching between grid-connected and island is realized effectively. Finally, experiments are carried out in Matlab/Simulink to verify the effectiveness and feasibility of the control strategy. The improved seamless switching control structure of BIC is shown on Fig. 9.

The parameters of seamless switching simulation experiment are shown in Table 1.

According to the requirements of control strategy algorithm, it is necessary to set the threshold of DC bus voltage and AC bus frequency. The rated value of DC bus voltage is 700V, and the threshold value is set as an upper maximum of 711V, an upper minimum of 701V, a lower maximum of 689V and a lower minimum of 699V. The rated of AC bus frequency is 50Hz, the threshold is set as the upper maximum of 50.06Hz, an upper minimum of 50.01Hz, a lower maximum of 49.94Hz, and a lower minimum of 49.99Hz.

In this paper, three group of experiments are used to demonstrate by comparison. The introduction of three groups of experiments is as follows: the first group, without adding pre-synchronization control, only the reference power switching algorithm is used to switch the mode directly. In the second group, pre-synchronization control and switching algorithm are added for mode switching. In the third group, the pre-synchronization and switching algorithm are added, and the disturbance observer is used to suppress the interference to achieve seamless switching. Due to the use of pure resistive resistance in the simulation process, the reactive power in AC/DC hybrid microgrid system is borne by AC sub-microgrid.

TABLE 1. Simulation experiment parameters.

Parameters	Symbol	Value	Unit
Rated voltage of AC bus	u_{ac}^{ref}	380	V
Rated frequency of AC bus	f^{ref}	50	Hz
Rated voltage of DC bus	u_{dc}^{ref}	700	V
AC sub-microgrid capacity	P_{dc}^{max}	10	kW
DC sub-microgrid capacity	P_{ac}^{max}	10	kW
Rated power of BIC	S	10	kVA
Filter inductor	L	5e-3	H
Filter resistor	R	0.01	Ω
Filter capacitor	C	1500e-6	F
Active power droop coefficient	m	1e-5	
Reactive power droop coefficient	n	3e-4	
D-axis DOB gain	l_d	5e-3	
Q-axis DOB gain	l_q	4e-2	

1) WITHOUT PRE-SYNCHRONIZATION CONTROL, GRID-CONNECTED/ISLAND MODE SWITCHING

Because the normal operation of microgrid needs to achieve accurate calculation of power, so in the process of microgrid operation, there must be a switching control algorithm of power calculation. Without pre-synchronization control, the simulation results are as follows.

0s-0.5s is the grid-connected mode, 0.5s-1.5s is the island mode, and the 1.5s-2.5s is the grid-connected mode. It can be seen from Fig. 10 that during the 1.5s switching from island mode to grid-connected mode, power mutation occurs, which seriously affects the stable operation of the two sub-microgrids and the public grid. The sudden change of power is caused by the large difference of frequency, phase and voltage amplitude between AC/DC hybrid microgrid system and public grid. The frequency, phase and voltage amplitude of AC side of BIC during mode switching are shown in Fig. 11.

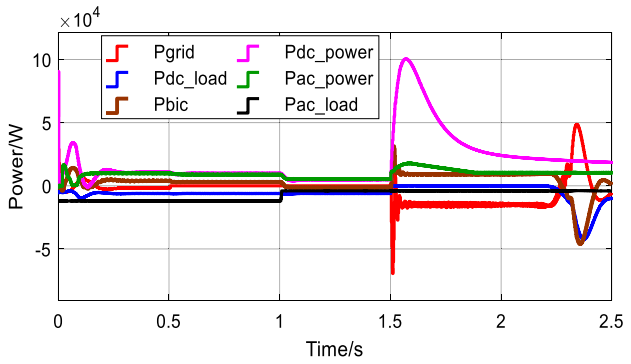

FIGURE 10. Active power transmission without pre-synchronization control.

It can be seen from Fig. 11(a) that after 1.5s grid-connected, the phase of BIC is still different from that public grid, and the phase synchronization has not been realized after 0.05s grid-connected. In Fig. 11(b), before 1.5s, the AC/DC hybrid microgrid switches from grid-connected mode to island mode. Because there is no control strategy, it can switch smoothly. When the island mode is switched to the grid-connected mode in 1.5s, the frequency jitter is more than 0.3Hz. In the later period of 1.6s-2s, although the frequency is stable at 50Hz, it is found that the power transmission has been disordered through Fig. 10. In Fig. 11(c), it can be seen that without the support of the public grid, the voltage amplitude will shift with the change of power. However, the voltage amplitude synchronization cannot be realized because there is no pre-synchronization control.

The disturbance of power will affect the stable operation of AC/DC sub-microgrid. After 1.5s, it will change from island mode to grid-connected mode. Because the AC sub-microgrid is supported by the public grid after grid-connected, the power of BIC will be directly transmitted to the public grid, and the frequency of DG is relatively stable, causing less impact. However, DC sub-microgrid and public grid seriously affected by the transmission power of BIC. The bus voltage of DC sub-microgrid is shown in Fig. 12.

It can be seen from Fig. 12 that when the island mode is switched to the grid-connected mode in 1.5s, the DC bus voltage drops instantaneously, and it cannot restore stability for a long time, which greatly affects the system stability. Further observer the influence of BIC and public grid A-phase voltage and current, as shown in Fig. 13.

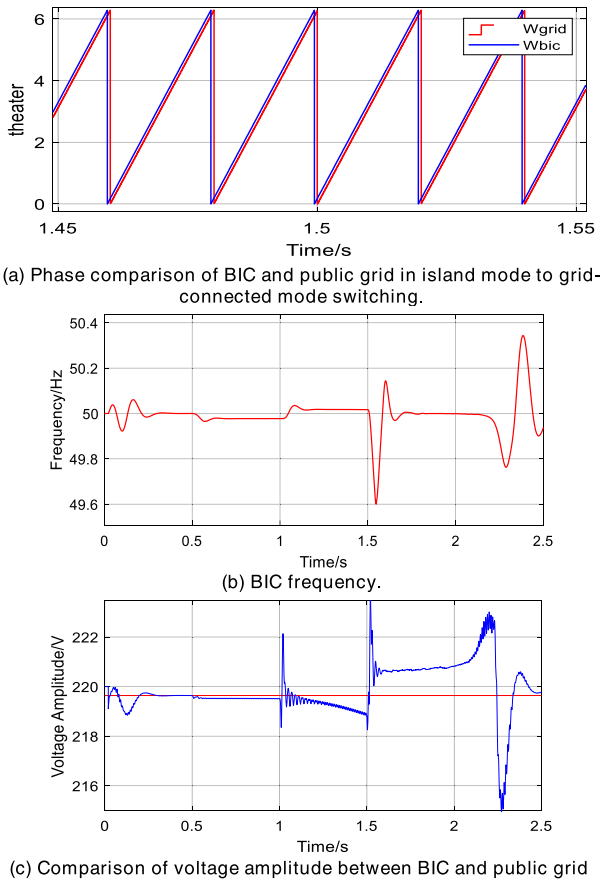

FIGURE 11. The parameter comparison between BIC and public grid without pre-synchronization control mode switching.

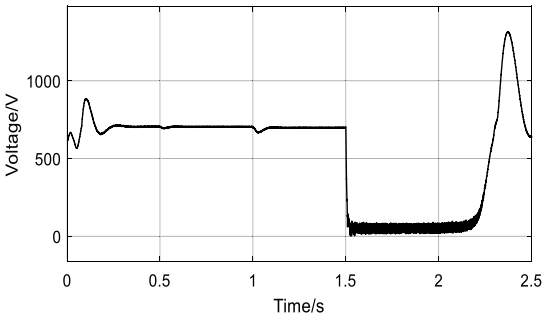

FIGURE 12. Bus voltage of DC sub-microgrid without pre-synchronization control.

In the process of switching from island mode to grid connected mode, A phase current fluctuates greatly. Theoretically, in the process of 1.5s-2s grid connected operation, the BIC transmits 4kW power to the public grid, which is the same as the process of 0s-0.5s grid connected operation. However, it can be seen from Fig. 13 that the A-phase current of 1.5s-2s BIC is unreasonable, and the microgrid system may collapse after 2s.

2) ADD PRE-SYNCHRONIZATION CONTROL MODE SWITCH

After adding the pre-synchronization control, the active power transmission is shown in Fig. 14.

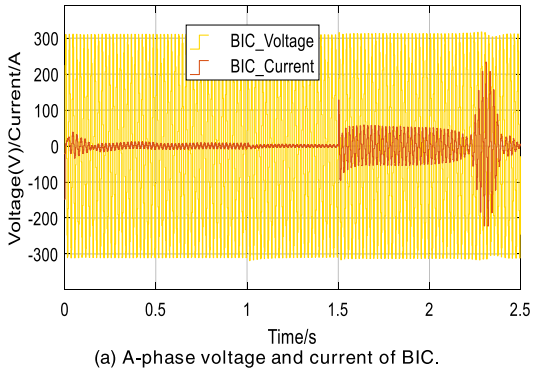

(a) A-phase voltage and current of BIC.

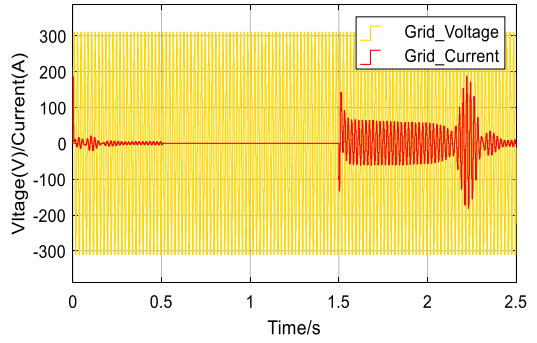

(b) A-phase voltage and current of public grid.

FIGURE 13. A-phase voltage and current in microgrid system without pre-synchronization control.

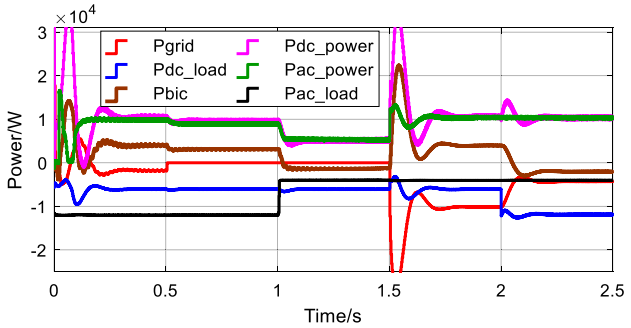

FIGURE 14. The active power transmission is controlled by pre-synchronization.

In Fig. 14, 0s-0.5s grid-connected operation, DC load is 6kW, and the residual power of DC sub-microgrid is 4kW, which is transmitted to the public grid through BIC. At this time, the BIC is in the inverter state. The AC load 12kW, and the AC sub-microgrid generates 10kW, so only 2kW of power flows into the public grid. 0.5s-1s, the grid-connected is switching to the island mode, because there is no control strategy switching, only involves the power calculation, so there will be no large fluctuations. At this time, the load does not change, without the support of the public grid, the AC/DC sub-microgrids should realize the load consumption sharing. DC sub-microgrid transmits 3kW power to AC sub-microgrid, BIC is in inverter state, AC sub-microgrid and DC sub-microgrid generates 9kW. When the AC load reduced to 4kW, the AC sub-microgrid transmits 1kW power to the DC sub-microgrid, the BIC is in rectification state, and power generation of the two sub-microgrid is 5kW.

1.5s-2s, from island mode to grid-connected mode, the load does not change, and the AC/DC sub-microgrid transmits the residual power to the public grid. At this time, the BIC is in the inverter state, and the public grid absorbs 10kW. In the 2s-2.5s grid-connected mode, the DC load increases to 12kW, and the supply of DC sub-microgrid is insufficient, so the public grid transmits 2kW power to DC side through BIC. The BIC is in rectification state, and the residual power of AC sub-microgrid is 6kW, so the public grid absorbs 4kW power.

Compared Fig.14 with Fig. 10 shows that there is no disturbance of power transmission after switching from island mode to grid-connected mode at 1.5s, only a large range of fluctuations exists. After mode switching, AC/DC hybrid microgrid can still achieve stable operation. For further comparative analysis, the phase, frequency and voltage amplitude after adding pre-synchronization control are shown in Fig. 15.

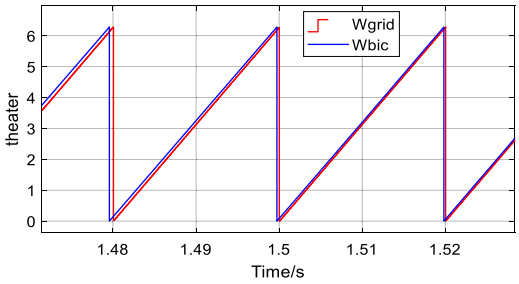

(a) Phase comparison of BIC and public grid in island mode to grid-connected mode switching.

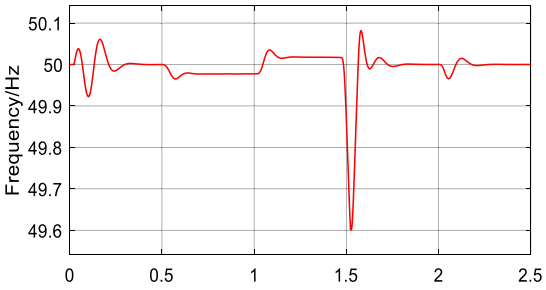

(b) BIC frequency.

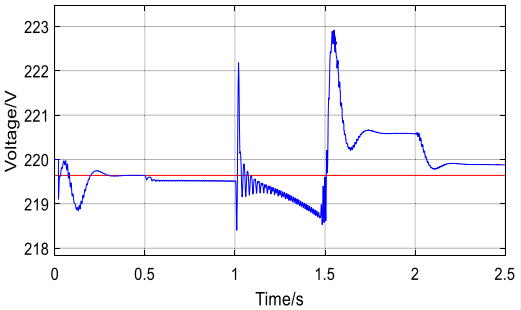

(c) Comparison of voltage amplitude between BIC and public grid.

FIGURE 15. The parameter comparison between BIC and public grid when pre-synchronization control mode switching is added.

In Fig. 15(a), the pre-synchronization control starts at 1.48s, and the phase is basically synchronized at 1.52s. In Fig. 15(b), after 1.5s mode switching, the frequency of BIC is gradually stabilized after experiencing large amplitude fluctuation, but the fluctuation amplitude is still large. In Fig. 15(c), after the 1.5s island mode is switched to grid-connected mode, although it can basically synchronize with the public grid, the voltage amplitude fluctuates greatly. At the same time, after adding per-synchronization control, the DC bus voltage is also improved, as shown in Fig. 16.

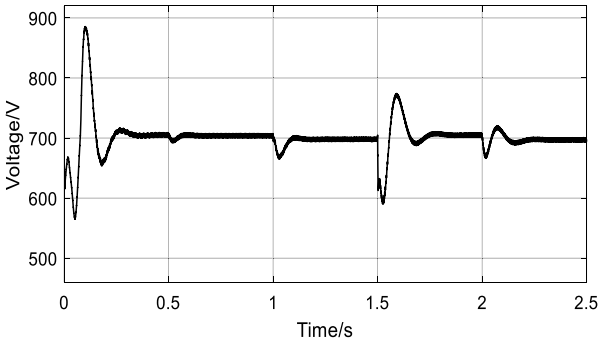

FIGURE 16. The bus voltage of DC sub-microgrid is controlled by pre-synchronization.

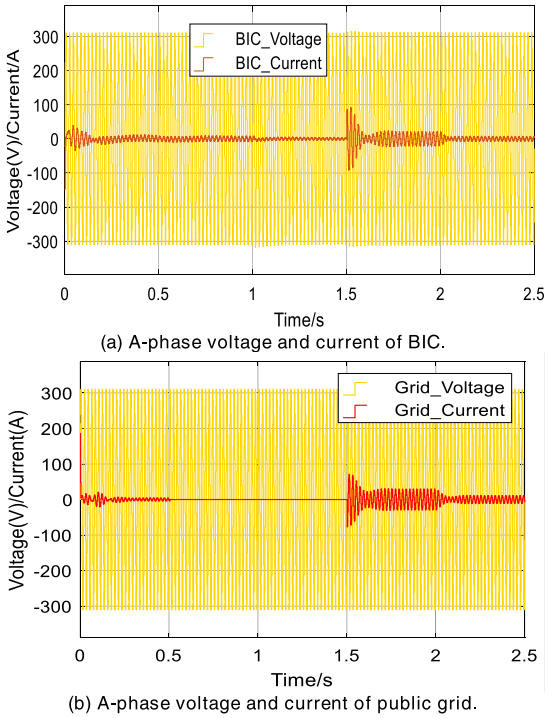

FIGURE 17. A-phase voltage and current in microgrid system with pre-synchronization control.

Compared Fig. 16 with Fig. 12, the DC bus voltage is still stable after fluctuation after 1.5s island mode switching to grid-connected mode, which indicates that the AC/DC sub-microgrids can achieve stable operation after mode switching after adding pre-synchronization control. The A-phase voltage and current of BIC and public grid are shown in Fig. 17.

3) MODE SWITCHING WITH PRE-SYNCHRONIZATION CONTROL AND DOB

Because of the large fluctuation in the mode switching process under the pre-synchronization control, the DOB is used for suppression and compensation. The active power transmission with pre-synchronization control and DOB is shown in Fig. 18.

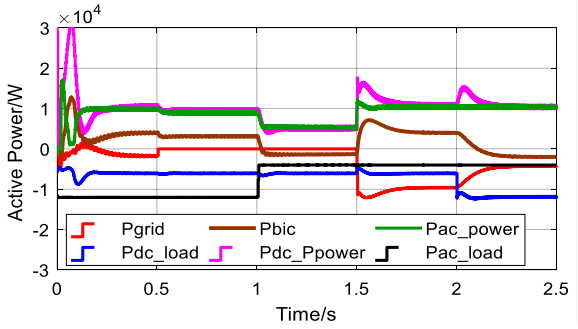

FIGURE 18. Add pre-synchronization control and DOB active power transmission.

Compared Fig.18 with Fig. 14, the active power transmission is significantly improved in the process of mode switching and load switching, especially in the 1.5s island mode to grid-connected mode switching. There is a large fluctuation in Fig. 14, and the power fluctuation in Fig.18 is relatively gentle. The fluctuation of AC bus frequency and DC bus voltage is also improved. The AC bus frequency is shown in Fig. 19.

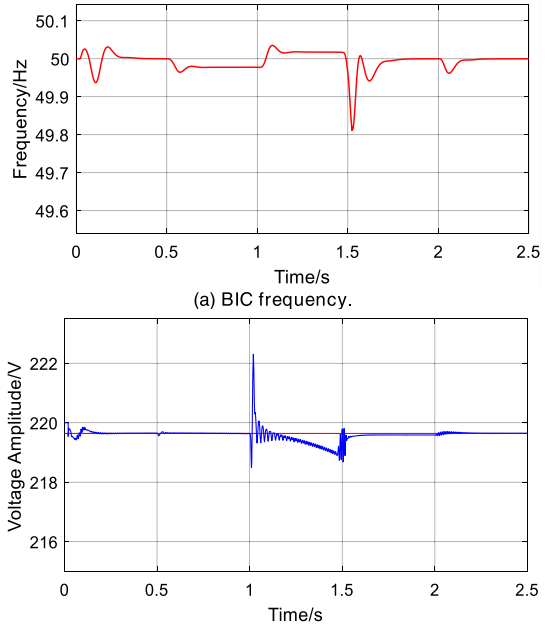

FIGURE 19. BIC frequency and voltage amplitude after adding pre-synchronization control and DOB.

As can be seen in Fig. 19(a), the maximum frequency fluctuation caused during the 1.5s island mode to grid-connected mode switching is about 0.19Hz, which is significantly reduce compared with the maximum value of 0.4Hz in Fig. 15(b). In Fig. 19(b), the voltage amplitude is basically consistent with the common voltage after switching from island mode to grid-connected mode. The frequency and voltage amplitude have been significantly improved, which is more in line with the standard of seamless switching. The DC bus voltage is shown in Fig. 20.

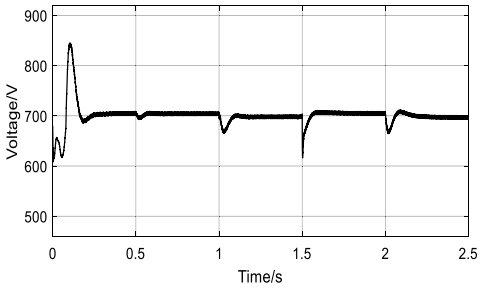

FIGURE 20. DC bus voltage after adding pre-synchronization control and DOB.

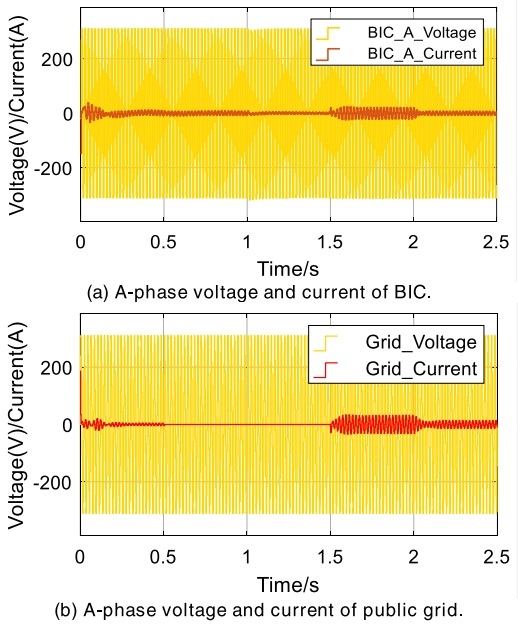

FIGURE 21. A-phase voltage and current in microgrid system with pre-synchronization control and DOB.

Compared Fig. 20 with Fig. 16, it can be seen that the voltage fluctuation amplitude is significantly reduced in the process of island mode to grid-connected mode switching. In Fig. 16, the lower limit of the peek amplitude of 1.5s island mode to grid-connected mode switching is about 590V, and the fluctuation amplitude is about 17%. In Fig. 20, the lower limit of 1.5s island mode to grid-connected mode switching fluctuation amplitude is about 630V, and the fluctuation amplitude is about 10%. According to the requirements of power quality voltage deviation, the deviation of DC bus voltage is within ±10% during stable operation. 0s-0.2s is the start-up stage of microgrid system, so the whole system meets the standard in the process of stable operation.

Finally, in the microgrid system with pre-synchronization control and DOB, the A-phase current and voltage of BIC and public grid are shown in Fig. 21.

Compared Fig. 21 with Fig. 17, in the process of switching from island mode to grid-connected mode, the current fluctuation in Fig. 21 is only small. Through the comparison of various parameters in the process of mode switching, the effectiveness and feasibility of the seamless switching control strategy based on pre-synchronization and DOB droop control are verified.

VI. CONCLUSION

A droop control strategy based on pre-synchronization and DOB is designed to achieve better switching between grid-connected and island operation modes of AC/DC hybrid microgrid. Through pre-synchronization control, the problem of power disorder and system collapse caused by the different of phase, frequency and voltage amplitude in the process of switching from island mode to grid-connected mode are solved. However, after adding the pre-synchronization control, there will still be large fluctuations in the process of mode switching. Therefore, DOB is added to the inner current loop of droop control to realize the suppression and compensation of interference through the estimation of disturbance current, so as to reduce the fluctuation in the system and realize the seamless switching.

REFERENCES

[1] X. Li, L. Guo, Y. Li, Z. Guo, C. Hong, Y. Zhang, and C. Wang, "A unified control for the DC–AC interlinking converters in hybrid AC/DC microgrids," *IEEE Trans. Smart Grid*, vol. 9, no. 6, pp. 6540–6553, Nov. 2018, doi: 10.1109/TSG.2017.2715371.

[2] A. Sajid, R. Sabzehgar, M. Rasouli, and P. Fajri, "Control of interlinking bidirectional converter in AC/DC hybrid microgrid operating in standalone mode," in *Proc. IEEE Milan PowerTech*, Milan, Italy, Jun. 2019, pp. 1–6, doi: 10.1109/PTC.2019.8810563.

[3] Z. Li and M. Shahidehpour, "Small-signal modeling and stability analysis of hybrid AC/DC microgrids," *IEEE Trans. Smart Grid*, vol. 10, no. 2, pp. 2080–2095, Mar. 2019, doi: 10.1109/TSG.2017.2788042.

[4] E. Aprilia, K. Meng, M. Al Hosani, H. H. Zeineldin, and Z. Y. Dong, "Unified power flow algorithm for standalone AC/DC hybrid microgrids," *IEEE Trans. Smart Grid*, vol. 10, no. 1, pp. 639–649, Jan. 2019, doi: 10.1109/TSG.2017.2749435.

[5] T. Uten, C. Charoenlarpnopparut, and P. Suksompong, "Synchronization control for microgrid seamless reconnection," in *Proc. 14th Int. Joint Symp. Artif. Intell. Natural Lang. Process. (iSAI-NLP)*, Chiang Mai, Thailand, Oct. 2019, pp. 1–6, doi: 10.1109/iSAI-NLP48611.2019.9045428.

[6] D. Q. Bi, W. Zhou, Y. X. Dai, and X. G. Li, "Control strategies of seamless switching for energy storage converter in hybrid AC/DC microgrid," *Autom. Electr. Power Syst.*, vol. 40, no. 10, pp. 84–89, May 2016.

[7] J. Zhang, Q. Wang, C. Hu, and T. Rui, "A new control strategy of seamless transfer between grid-connected and islanding operation for microgrid," in *Proc. 12th IEEE Conf. Ind. Electron. Appl. (ICIEA)*, Siem Reap, Cambodia, Jun. 2017, pp. 1729–1732, doi: 10.1109/ICIEA.2017.8283118.

[8] Y. Shi, J. D. Lai, J. W. Su, X. Z. Yang, W. J. Wu, and Y. Du, "Control strategy of seamless transfer for microgrid operation mode," *Autom. Electr. Power Syst.*, vol. 40, no. 8, pp. 85–91, Apr. 2016.

[9] M. Amin and Q.-C. Zhong, "Resynchronization of distributed generation based on the universal droop controller for seamless transfer between operation modes," *IEEE Trans. Ind. Electron.*, vol. 67, no. 9, pp. 7574–7582, Sep. 2020, doi: 10.1109/TIE.2019.2942556.
[10] X. Hou, Y. Sun, J. Lu, X. Zhang, L. H. Koh, M. Su, and J. M. Guerrero, "Distributed hierarchical control of AC microgrid operating in grid-connected, islanded and their transition modes," *IEEE Access*, vol. 6, pp. 77388–77401, 2018, doi: 10.1109/ACCESS.2018.2882678.
[11] Y. Li, L. Fu, K. Meng, Z. Y. Dong, K. Muttaqi, and W. Du, "Autonomous control strategy for microgrid operating modes smooth transition," *IEEE Access*, vol. 8, pp. 142159–142172, 2020, doi: 10.1109/ACCESS.2020.3014255.
[12] M. Ganjian-Aboukheili, M. Shahabi, Q. Shafiee, and J. M. Guerrero, "Seamless transition of microgrids operation from grid-connected to islanded mode," *IEEE Trans. Smart Grid*, vol. 11, no. 3, pp. 2106–2114, May 2020, doi: 10.1109/TSG.2019.2947651.
[13] J. Yang, S. Li, and X. Yu, "Sliding-mode control for systems with mismatched uncertainties via a disturbance observer," *IEEE Trans. Ind. Electron.*, vol. 60, no. 1, pp. 160–169, Jan. 2013, doi: 10.1109/TIE.2012.2183841.
[14] J. W. Chen, S. C. Hou, and J. Chen, "Seamless mode transfer control for a master-slave microgrid," in *Proc. 44th Annu. Conf. IEEE Ind. Electron. Soc. (IECON)*, Washington, DC, USA, Oct. 2018, pp. 255–259.
[15] C. N. Papadimitriou, V. A. Kleftakis, and N. D. Hatziargyriou, "Control strategy for seamless transition from islanded to interconnected operation mode of microgrids," *J. Mod. Power Syst. Clean Energy*, vol. 5, no. 2, pp. 169–176, Mar. 2017, doi: 10.1007/s40565-016-0229-0.
[16] L. Zacharia, A. Kyriakou, L. Hadjidemetriou, E. Kyriakides, C. Panayiotou, B. Azzopardi, N. Martensen, and N. Borg, "Islanding and resynchronization procedure of a university campus microgrid," in *Proc. Int. Conf. Smart Energy Syst. Technol. (SEST)*, Seville, Spain, Sep. 2018, pp. 1–6, doi: 10.1109/SEST.2018.8495828.
[17] Z. W. Liu, S. H. Miao, Z. H. Fan, Y. L. Kang, K. Y. Chao, and D. D. Sun, "Power control and voltage fluctuation suppression strategy of the bidirectional AC/DC converter in the island hybrid microgrid," *Proc. Chin. Soc. Electr. Eng.*, vol. 39, no. 21, pp. 6225–6237, 2019.

GUISHUO WANG (Fellow, IEEE) received the B.S. degree in communication engineering from Taishan University, Taian, China, in 2017. He is currently pursuing the M.E. degree in electronics and communications engineering with Shandong University. His research interests include ac/dc hybrid microgrid, interlinking converter, and control strategy.

XIAOLI WANG received the B.E. degree in electronic science and technology from Shandong University, Weihai, China, and the M.E. degree in circuits and systems from Shandong University, Jinan, China. He is currently a Senior Experimentalist and a Supervisor of master's student with Shandong University. His current research interests include ac/dc hybrid microgrid, smart grid, and Internet of Things wireless communication.

XIANG GAO received the B.S. degree in electronic information science and technology from Shandong University, Weihai, China, in 2006, and the M.E. and Ph.D. degrees in communication engineering from the Korea University of Technology and Education, Cheonnan, South Korea, in 2008 and 2012, respectively. He is currently a Lecturer and a Supervisor of master's students with Shandong University. His research interests include Internet of Things technology, cognitive radio, and quantum communication.